



# Comparison of mechanical and tribological properties of glass-fiber-reinforced polyketone and polyketone/polyamide 6 blend composites

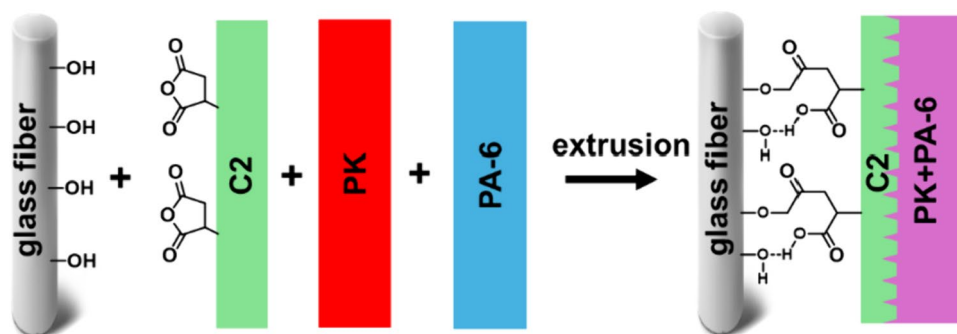
Irem Nehir Uysal<sup>1,2</sup> · Mehmet Atilla Tasdelen<sup>1</sup>

Received: 17 November 2023 / Revised: 5 March 2024 / Accepted: 6 March 2024 / Published online: 8 April 2024  
© The Author(s), under exclusive licence to The Polymer Society of Korea 2024

## Abstract

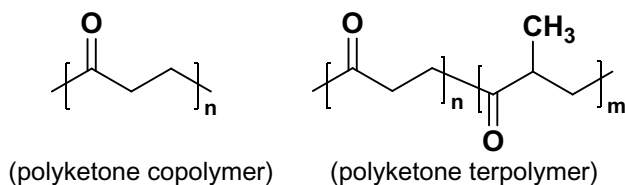
In this study, the impact of two compatibilizers, ethylene terpolymer (C1) and maleic anhydride grafted polyethylene (C2), on the mechanical, thermal, and tribological properties of 30% glass-fiber-reinforced polyketone (PK) and polyketone/polyamide 6 (PK/PA-6) blend composites was investigated. In the case of 30% glass-fiber-reinforced PK composites, the mechanical test results showed that C2 significantly improves the impact resistance (over 48.8%) and elongation at break (over 13.3%) values due to the enhanced compatibility between glass fibers and the PK matrix, attributed to the maleic anhydride functionality. The tensile and flexural properties of the 30% glass-fiber-reinforced PK/PA-6 blend composites were determined to be between the values of pure PK/GF30 and PA-6/GF30 composites, which were its constituent components. Notably, these blend composites displayed higher impact resistance (19.6 kJ/m<sup>2</sup>) and elongation at break (4.86%) values than the pure PK/GF30 and PA-6/GF30 composites. The SEM images suggested that C2 creates a better interface between glass fibers and the matrix, resulting in a more cohesive structure. Differential scanning calorimeter analysis revealed two distinct glass transition temperatures, indicating the existence of two phases, and reflecting the immiscibility of the two polymers. Tribological studies showed that the friction coefficients and specific wear rates of PK/PA-6/GF30 composites were improved by increasing PK segment. The PK-25/PA6-50/GF30-C2 sample exhibited a friction coefficient of 0.341  $\mu$  and a specific wear rate of 1.15 10<sup>-6</sup> mm<sup>3</sup>/Nm. Overall, the C2 proved to be a more suitable compatibilizer than C1, offering valuable insights for tailoring high-performance materials with enhanced properties.

## Graphical Abstract



The influence of two compatibilizers, ethylene terpolymer (C1) and maleic anhydride grafted polyethylene (C2), on the mechanical, thermal, and tribological properties of 30% glass-fiber-reinforced polyketone and polyketone/polyamide 6 blend composites was investigated. Based on, mechanical, microscopic, thermal, and tribological results, the C2 was found to be a more suitable compatibilizer than C1 for improving the interface between glass fibers and the matrix

**Keywords** Blends · Composites · Glass fiber · Polyamides · Polyketones · Tribological properties



**Scheme 1.** Chemical structures of aliphatic polyketone copolymer and terpolymer

## 1 Introduction

Aliphatic polyketones (PKs) are high-performance engineering thermoplastics produced from relatively inexpensive starting materials  $\alpha$ -olefins (especially ethylene) and carbon monoxide as an air pollutant. Two types of PKs, including copolymers and terpolymers, whose chemical structures are presented in Scheme 1, are commercially available. They are produced by alternating copolymerization of carbon monoxide with either ethylene or a combination of ethylene and propylene. Incorporating propylene into the copolymer reduces both the structural regularity of the chain and the melting and processing temperatures. Compared to other common thermoplastics, the PKs exhibit high heat resistance and can withstand elevated temperatures without significant degradation, making them suitable for applications requiring thermal stability [1]. In addition, they can be easily shaped using conventional processing techniques like injection molding, extrusion, and blow molding that enhance their potential uses in various applications. While polyketones possess numerous desirable properties, they also have some drawbacks, such as moisture sensitivity, long-term stability, adhesion and bonding, aesthetics, and limited availability and color range that should be considered in their application. Owing to these drawbacks, they can be blended with commercially available polymers to enhance their properties, performance, expand their application range, and achieve cost saving. In the literature, polyketones are frequently blended with other synthetic polymers [2], including polyamides (polyamide 6 (PA-6) [3–9] and polyamide 12 [10]), polypropylene [11, 12], polylactic acid [13], polyvinyl chloride [14], ethylene vinyl alcohol copolymer (EVOH) [15], and polycarbonate [16, 17]. The melt blending by extrusion is an efficient process that offers many advantages in terms of material quality, productivity, and cost-effectiveness, creating novel polymeric materials with a combination of desirable characteristics [18–20]. In the case of PK, the PA are partially miscible with PK, which makes it an ideal candidate for the melt blending with PK toward high-performance materials [21]. The PK exhibits higher chemical resistance (surpassing PAs by more than

30%), impact resistance (exceeding PAs by over 230%), and abrasion resistance (being 14 times better than polyoxymethylene) to among many other plastic materials [22]. Due to the limited chemical attraction between the polymeric components, the manufacturing of their blends resulted in a multiphase system. To overcome this issue, the addition of compatibilizers effectively promotes the formation of physical or chemical bonds between the two phases allowing finer dispersion of immiscible polymers [23, 24]. Recently, the morphological changes of the PK/PA-6 blend were investigated by Asona et al. under both dry and wet conditions. They reported that PK/PA-6 blend displayed a complex morphology consisting of crystalline lamellae and spherical and cylindrical domains. Surprisingly, the obtained PK/PA-6 blends (PK/PA-6 = 70:30 or 60:40 wt %) exhibited higher Izod impact strength under wet conditions (ranging from 150 to 200 kJ m<sup>-2</sup>) than dry conditions (less than 50 kJ m<sup>-2</sup>) [3, 4]. In another study, melt blending of PK and EVOH was conducted to enhance oxygen barrier properties and film characteristics for flexible packaging applications. The resulting PK/EVOH blend films not only demonstrate exceptional oxygen barrier properties but also exhibit superior stretching characteristics, which are valuable for food packaging [15].

The aim of this study is to investigate melt blending of PK and PA-6 having similar melting temperatures with a consistent glass-fiber ratio of 30% by weight. Two different compatibilizers, namely, ethylene terpolymer (C1) and maleic anhydride grafted polyethylene (C2), are examined to improve interfacial interactions between the PK and PK/PA-6 polymer blend with the glass fiber. Additionally, the influence of blend ratios on the mechanical, thermal, and tribological properties of 30% glass-fiber-reinforced PK and PK/PA-6 blend composites is also investigated by a co-rotating twin screw extruder. Test samples were manufactured through the injection molding method and their mechanical properties are assessed through tensile, flexural, and Izod impact tests under load. Subsequently, the surfaces of the fractured samples following mechanical tests are examined using a scanning electron microscope to determine fiber–matrix interactions. Finally, the thermal and tribological properties of the composites are investigated based on differential scanning calorimetry and wear tests.

## 2 Experimental

### 2.1 Materials

The aliphatic PK terpolymer (Poketone, M630A) and PA-6 (Durethan B26) used in this study were purchased from Hyosung Corp. (Korea) and Lanxess GmbH (Germany), respectively. Their technical data are summarized

**Table 1** Physical properties of PK and PA-6

Parameters and units	Test methods	PK	PA-6
Density (g/cm <sup>3</sup> )	ISO 1183	1.24	1.14
Tensile modulus (MPa)	ISO 527-1,-2	1450	3000
Tensile strength at yield (MPa)	ISO 527-1,-2	60	75
Elongation at break (%)	ISO 527-1,-2	300	15
Flexural modulus (MPa)	ISO 178-A	1500	2700
Flexural strength (MPa)	ISO 178-A	57	100
Charpy impact strength (kJ/m <sup>2</sup> )	ISO 179/1eA	7	< 10
Melting temperature (°C)	ISO 11357-1,-3	222	222
Vicat softening temperature (°C)	ISO 306	195	200
Melt flow index (g/10 min)	ISO 1133	6	–

in Table 1. The PK and PK/PA-6 composites were prepared with two types of E-glass fibers added at an amount of 30 wt % and obtained from Jushi Group (Zhejiang, China): the 534A-type fibers (filament diameter = 11 μm, chop length = 4.5 mm, size content = 0.7%, moisture content = ≤ 0.10%) were treated with a silane-based sizing, compatible with poly(ethylene terephthalate) and poly(butylene terephthalate) and the 568H-type fibers (filament diameter = 11 μm, chop length = 4.5 mm, size content = 0.45%, and moisture content = ≤ 0.10%) were treated with a silane-based sizing, compatible with PA-6 and PA-66.

The ethylene terpolymer (C1, Dow Chemical, USA,  $d = 0.94 \text{ g/cm}^3$ , melting temperature = 72 °C, and melt flow index = 12 g/10 min) and maleic anhydride grafted polyethylene (C2, Dow Chemical, USA,  $d = 0.875 \text{ g/cm}^3$ , maleic anhydride content = 0.5–1 wt%, melting temperature = 63 °C, and melt flow index = 1.3 g/10 min) were used as compatibilizers, while zinc stearate (Akdeniz Chemson Additives Inc., Turkey) was used as a lubricant.

## 2.2 Preparation of composites

The glass-fiber-reinforced PK and PK/PA 6 composites were prepared by a co-rotating twin screw extruder (COPERION ZSK 26). The materials were mixed at temperature profiles of 180 to 230 °C and processed at a screw rotation speed of 350 rpm. All details about formulations and sample codes are listed in Table 2. Produced composite granules were molded by injection process according to ISO 527 and ISO 179 standards for the tensile, bending, and impact tests. Five test specimens were made to determine the average value of each mechanical data.

## 2.3 Characterization

A universal tester (Zwick Z020 Universal Testing Machine) was used to analyze tensile and flexural properties of glass-fiber-reinforced composites. The load cell used was 5 kN and the crosshead speed for the measurements was fixed at 10 mm/min. All measurements were performed, at room temperature, on dog-bone shaped tensile bars having dimensions according to ISO 527:2019 and ISO 1178:2019 standards. The notched Izod impact tests were performed based on ISO 180:2023 standard with an Instron CEAST 9050 model impact testing machine. Differential scanning calorimeter (DSC) analyses were performed using Netzsch DSC 214 in nitrogen atmosphere. The analysis was conducted from 30 °C to 250 °C with a heating rate of 10 °C/min. The tribological behaviors of all the composites were examined by a pin on disk wear test instrument (UTS Tribolog, Turkey) followed by ASTM-G99-23 standard. The wear test was performed with the pin (size of about 20 mm diameter and 30 mm length) at room temperature, room humidity, and pressure. The wear tests were carried out under 40 N load, at 400-rpm sliding speed, and 5000 m sliding distance. During the wear tests, wear track profiles of the hybrid composites were obtained according to the scanned distance and wear depth.

**Table 2** Codes and formulation details of glass-fiber-reinforced PK and PK/PA 6 composites

Sample	PK (wt%)	PA-6 (wt%)	GF (wt%)	Comp (wt%)	Lub <sup>c</sup> (wt%)	Total (wt%)
PK/GF30	69.7	–	30	–	0.3	100
PK/GF30-C1 <sup>a</sup>	66.7	–	30	3	0.3	100
PK/GF30-C2 <sup>b</sup>	66.7	–	30	3	0.3	100
PA/GF30	69.7	–	30	–	0.5	100
PK-15/PA6-50/GF30- C1	15	49.5	30	5	0.5	100
PK-25/PA6-40/GF30- C1	25	39.5	30	5	0.5	100
PK-15/PA6-50/GF30- C2	15	49.5	30	5	0.5	100
PK-25/PA6-40/GF30- C2	25	39.5	30	5	0.5	100

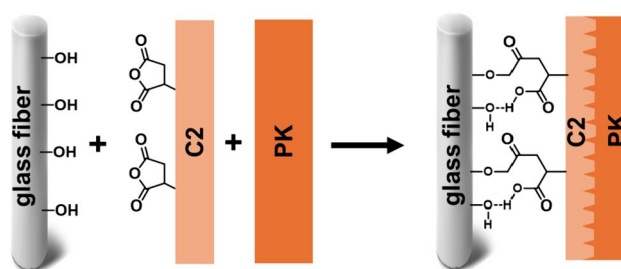
<sup>a</sup>Compatibilizer 1 (C1): ethylene terpolymer. <sup>b</sup>Compatibilizer 2 (C2): maleic anhydride grafted polyethylene. <sup>c</sup>Zinc stearate was used as a lubricant

### 3 Results and discussion

#### 3.1 Mechanical properties

The tensile, flexural, and Izod impact test results are summarized in Table 3. The addition of ethylene terpolymer in the PK/GF30 composite resulted in a decrease in both tensile and flexural modulus as well as tensile and flexural strength, while the elongation at break and notched Izod impact strength were slightly increased. On the other hand, the mechanical properties including tensile (7.3%), flexural (7.8%), and notched Izod impact (48.8%) strengths, along with elongation at break (13.3%) values of PK/GF30 were remarkably improved in the PK/GF30 composite using maleic anhydride grafted polyethylene (C2). However, its tensile (9.9%) and flexural (19.3%) modulus values were lower than those of the pristine PK/GF30 composite. As a result, the PK/GF30 composites exhibited a significant improvement in impact resistance over 48.8% with the addition of 3 wt % C2 compatibilizer. This improvement was limited to only 2.4% for the PK/GF30-C1 sample containing ethylene terpolymer compatibilizer. Therefore, it was concluded that the compatibility of the C2 was more appropriate than the C1 for the preparation of glass-fiber-reinforced PK composites (Scheme 2).

The interaction between the glass fiber and the PK matrix was investigated by scanning electron microscopy (SEM) from the fractured surface of samples after the tensile tests (Fig. 1). In all SEM images, it was observed that the glass fiber was randomly dispersed in the PK matrix. When comparing the SEM images of PK/GF30-C1 with PK/GF30-C2, it was evident that the surfaces of the glass fibers were coated with a thin layer of the matrix material when C2 was used as a compatibilizer. As previously noted, the compatibility between PK matrix and glass fiber was inherently restricted due to the distinct nature of their surface properties. During the melt blending, the maleic anhydride functionality of C2 could react with the hydroxyl groups on the glass fiber, thereby reducing its surface polarity. Therefore, the interfacial bonding between glass fiber and the PK matrix as well as their



**Scheme 2.** Proposed intermolecular interactions between glass fiber, C2, and polyketone matrix

compatibility, were significantly improved with the use of the C2 compatibilizer (Scheme 2). [25]

The melt blending of PK with polyamide 6 (PA), reinforced with 30% glass fiber, was also investigated in the presence of C1 and C2 compatibilizers. Two different blending ratios of PK/PA-6/GF/compatibilizer were utilized with weight percentages of 15/50/30/5 and 25/40/30/5. The effects of the type of compatibilizer and blending ratio on the mechanical, thermal, and tribological properties of the resulting composites were investigated. The mechanical properties of the 30% glass-fiber-reinforced PK/PA-6 blend composites obtained from tensile, flexural, and Izod impact tests were summarized in Table 4. The tensile and flexural modulus, as well as the tensile and flexural strength values of PK/PA-6/GF30 blend composites were within the range of values observed for both the neat PK/GF30 and PA-6/GF30 composites. The maximum improvements in tensile and flexural modulus were recorded as  $9.3 \pm 0.12$  and  $7.5 \pm 0.27$  GPa for the PK-15/PA6-50/GF30-C2 sample, respectively, representing approximately 31% and 32% increases compared to the control sample (PK/GF30). However, these values were significantly lower than the values of the neat PA-6/GF30 sample. On the other hand, all blend composites showed a remarkable increase in impact strength and elongation at break values. The Izod impact values of the neat PK/GF30 and PA-6/GF30 composites improved by 139% and 74%, respectively, following the formation of the PK-15/PA6-50/GF30-C2 sample. In contrast, the maximum elongation at break value was determined as  $4.86 \pm 0.04\%$  for the PK-25/PA6-40/GF30-C2 sample, which was approximately 115%

**Table 3** Mechanical properties of 30% glass-fiber-reinforced PK composites

Sample	Tensile modulus (GPa)	Tensile strength at yield (MPa)	Elongation at break (%)	Flexural modulus (GPa)	Flexural strength (MPa)	Izod impact strength (kJ/m <sup>2</sup> )
PK/GF30	$7.1 \pm 0.21$	$82 \pm 1.33$	$2.26 \pm 0.42$	$5.7 \pm 0.08$	$116 \pm 3.78$	$8.2 \pm 0.24$
PK/GF30-C1	$6.5 \pm 0.07$	$53 \pm 0.67$	$2.43 \pm 0.22$	$5.2 \pm 0.21$	$83 \pm 0.78$	$8.4 \pm 0.11$
PK/GF30-C2	$6.4 \pm 0.23$	$88 \pm 2.13$	$2.56 \pm 0.11$	$4.6 \pm 0.03$	$125 \pm 3.55$	$12.2 \pm 0.24$

All tests were conducted five times to confirm reproducibility

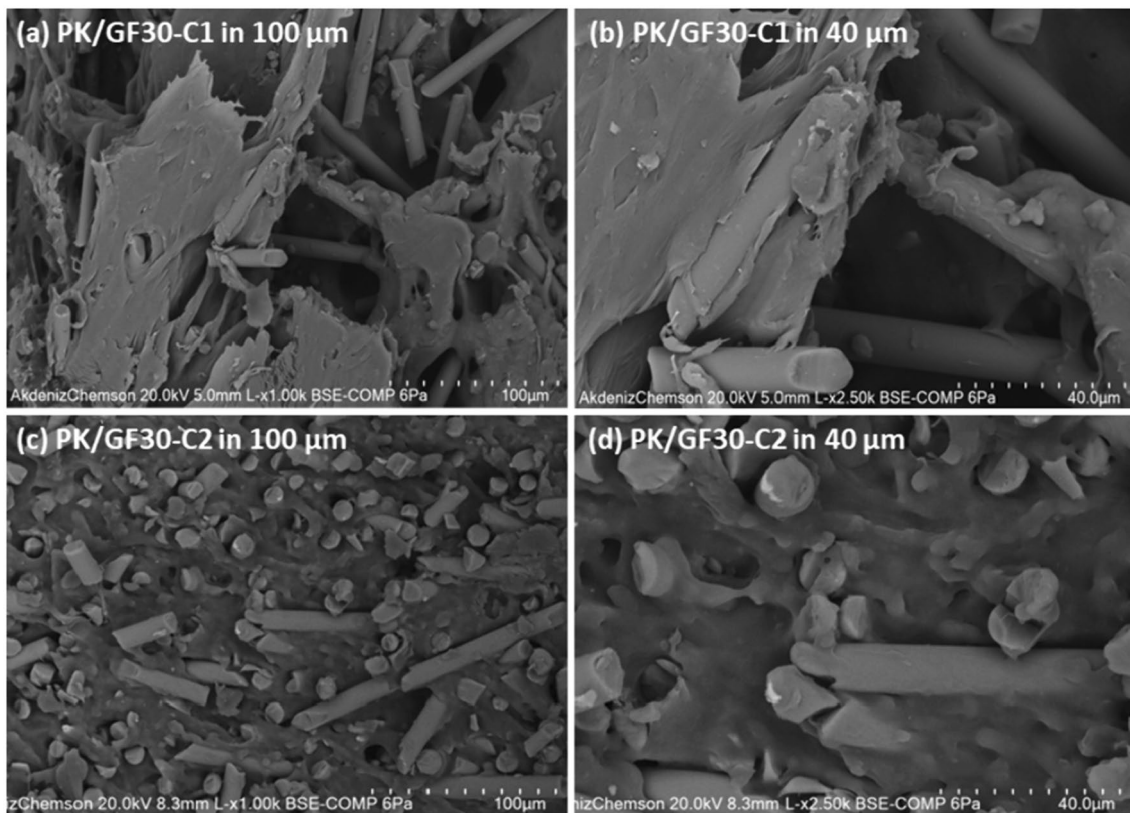


**Fig. 1** SEM images of PK/GF30-C1 in 100  $\mu\text{m}$  (a) and in 40  $\mu\text{m}$  (b), and PK/GF30-C2 in 100  $\mu\text{m}$  (c) and in 40  $\mu\text{m}$  (d)

**Table 4** Mechanical properties of 30% glass-fiber-reinforced PK/GF30, PA-6/GF30, and PK/PA-6 blend composites

Sample	Tensile modulus (GPa)	Tensile strength at yield (MPa)	Elongation at break (%)	Flexural modulus (GPa)	Flexural strength (MPa)	Izod impact strength (kJ/m <sup>2</sup> )
PK/GF30	$7.1 \pm 0.21$	$82 \pm 1.33$	$2.26 \pm 0.42$	$5.7 \pm 0.08$	$116 \pm 3.78$	$8.2 \pm 0.24$
PA-6/GF30	$10.6 \pm 0.18$	$168 \pm 2.67$	$3.00 \pm 0.09$	$8.3 \pm 0.16$	$266 \pm 2.65$	$11.3 \pm 0.18$
PK-15/PA6-50/ GF30-C1	$8.2 \pm 0.08$	$123 \pm 0.89$	$3.76 \pm 0.04$	$6.8 \pm 0.13$	$197 \pm 2.08$	$16.5 \pm 0.31$
PK-25/PA6-40/ GF30-C1	$8.2 \pm 0.17$	$126 \pm 1.11$	$4.50 \pm 0.13$	$6.9 \pm 0.07$	$218 \pm 0.58$	$16.5 \pm 0.30$
PK-15/PA6-50/ GF30-C2	$9.3 \pm 0.12$	$144 \pm 0.44$	$4.26 \pm 0.35$	$7.5 \pm 0.27$	$225 \pm 2.00$	$19.6 \pm 0.10$
PK-25/PA6-40/ GF30-C2	$8.4 \pm 0.14$	$130 \pm 0.44$	$4.86 \pm 0.04$	$6.5 \pm 0.01$	$200 \pm 2.08$	$17.3 \pm 0.23$

All tests were conducted five times to confirm reproducibility

and 62% higher than the values of the neat PK/GF30 and PA-6/GF30 composites.

The mechanical properties of blend composites with C1 compatibilizer, including tensile modulus and strength, elongation at break, flexural modulus and strength, and Izod impact strength, were relatively consistent when increasing the PK feed ratio from 15 to 25%. In the SEM images, it was observed that the glass fibers were randomly distributed throughout the polymer matrix in both the 15% and 25% PK feed ratio samples (Fig. 2). This indicated a well-mixed blend, and it is clear that the glass fibers effectively

contribute to the composite's strength. However, the interface between the glass fibers and the polymer matrix appeared relatively smooth and exhibited weak bonding leading instances of local fiber debonding. Consequently, the presence of fiber pullout suggested that the interface strength could be further optimized, potentially by changing the type of compatibilizer.

After the use of maleic anhydride based-compatibilizer (C2), a highly uniform and well-dispersed distribution of glass fibers within the PK/PA-6 matrix was observed (Fig. 3). All fibers were randomly distributed, demonstrating

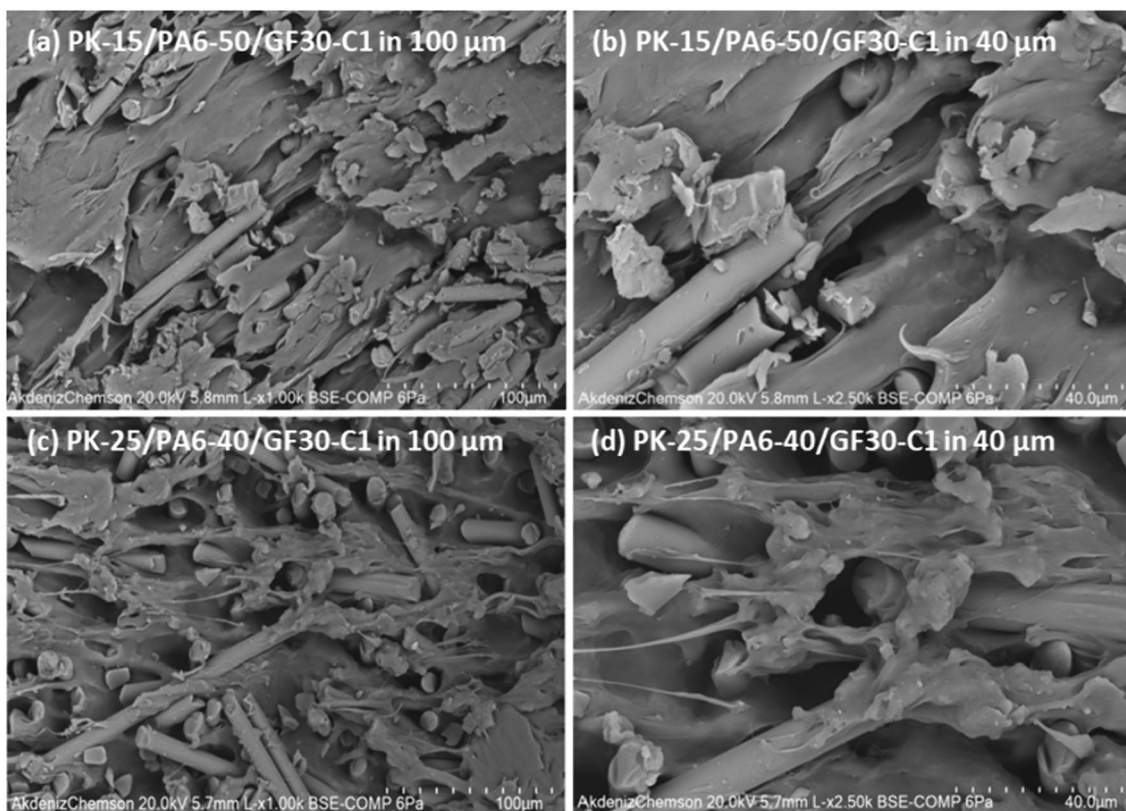


**Fig. 2** SEM images of PK-15/PA6-50/GF30-C1 in 100  $\mu\text{m}$  (a) and in 40  $\mu\text{m}$  (b), and PK-25/PA6-40/GF30-C1 in 100  $\mu\text{m}$  (c) and in 40  $\mu\text{m}$  (d)

effective mixing during the blending process. The interface between the glass fibers and the matrix appeared highly cohesive, resulting in minimal instances of fiber pullout. The strong fiber-matrix interface and overall microstructural integrity significantly improved the impact strength and elongation at break values of the composite. The mechanical test including tensile, flexural, and Izod impact showed that the PK-25/PA6-40/GF30-C2 composite with a 25% PK feed ratio exhibited distinctly lower mechanical properties compared to the PK-15/PA6-50/GF30-C2 sample (Table 4). A change in the blend ratio could alter the interaction between the two polymers, potentially affecting mechanical properties of the composites. In the PK-25/PA6-40/GF30-C2 sample, the higher proportion of PK resulted in a stiffer and less ductile matrix, potentially leading to reduced tensile and flexural strength.

### 3.2 Thermal properties

The thermal behavior of the PK/GF-30-C1 and PK/GF-30-C2 samples was investigated by DSC with a heating rate of 10  $^{\circ}\text{C}/\text{min}$  between 0 and 250  $^{\circ}\text{C}$  under nitrogen atmosphere. The neat aliphatic PK terpolymer (Poketone, M630A) and PA-6 (Durethan B26) exhibited 15 and 52  $^{\circ}\text{C}$  as the glass transition temperature ( $T_g$ ) and 222  $^{\circ}\text{C}$  (hangisi için?) as the

melting temperature ( $T_m$ ), respectively. After the preparation of 30% glass-fiber-reinforced composites in the presence C1 and C2 compatibilizers, a slight decrease was recorded in both  $T_g$  and  $T_m$  values of PK/GF-30 and PA-6/GF-30 samples. The addition of compatibilizer increased the segmental mobility of the polymer chains and the free volume between the polymer chain, resulting in a slight decrease of the  $T_g$  and  $T_m$  values of PK/GF-30 and PA-6/GF-30 samples.

The influence of feed ratio of PK/PA-6 and type of compatibilizer on the  $T_g$  and  $T_m$  values of 30% glass-fiber-reinforced blend composites was also investigated by DSC. As shown in Fig. 4a and Table 5, the  $T_g$  of the PK phase increased slightly, whereas the  $T_g$  of the PA-6 phase decreased from 50.4 and 49.9  $^{\circ}\text{C}$  to 48.7 and 48.5  $^{\circ}\text{C}$ , respectively, as the PK content increased from 15 to 25%. The presence of two distinct  $T_g$ s indicated the existence of two phases and reflected the immiscibility of the two polymers [26, 27]. It was also noted that the effect of the C2 compatibilizer on  $T_g$  change was more pronounced compared to the C1 compatibilizer. This could be attributed to the presence of maleic anhydride functionality in the C2 compatibilizer promoting better adhesion between the two phases. In the case of  $T_m$  30% glass-fiber-reinforced blend composites, a single peak for the  $T_m$  was observed, because the  $T_m$  values of the two phases ( $T_{m\text{PK}}$  and  $T_{m\text{PA-6}} = 222$   $^{\circ}\text{C}$ )

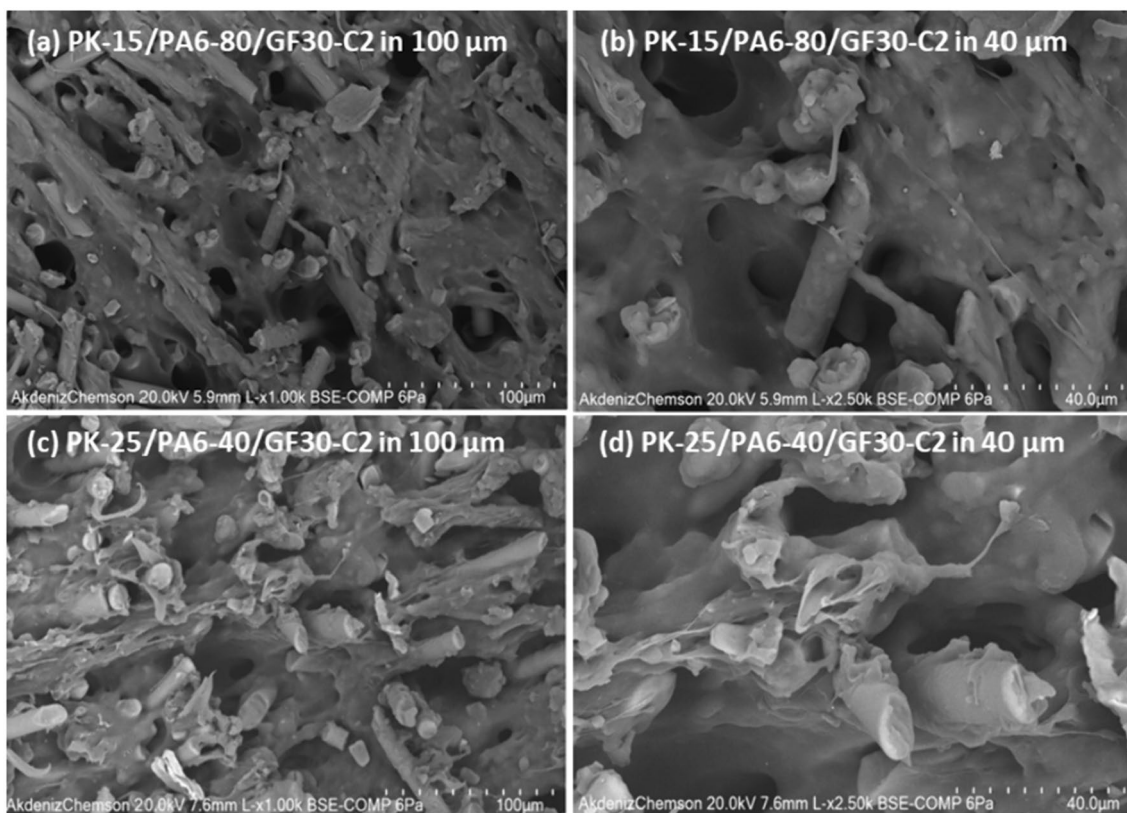


Fig. 3 SEM images of PK-15/PA6-80/GF30-C2 in 100 μm (a) and in 40 μm (b), and PK-25/PA6-40/GF30-C2 in 100 μm (c) and in 40 μm (d)

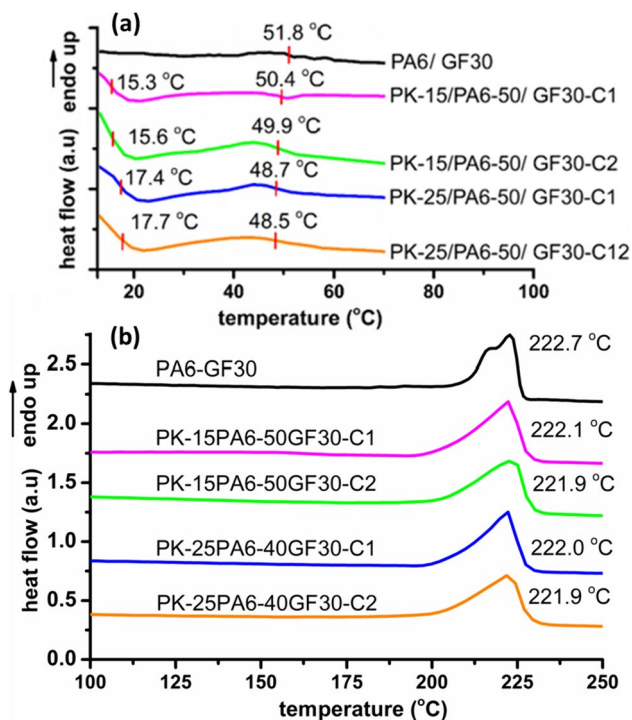


Fig. 4 DSC thermograms of PA6/GF30, PK-15/PA6-50/GF30-C1, PK-25/PA6-40/GF30-C1, PK-15/PA6-50/GF30-C2, and PK-25/PA6-40/GF30-C2 samples

were very close, and both peaks overlapped (Fig. 4b). Additionally, no significant change in  $T_m$  values was observed in all blend composites.

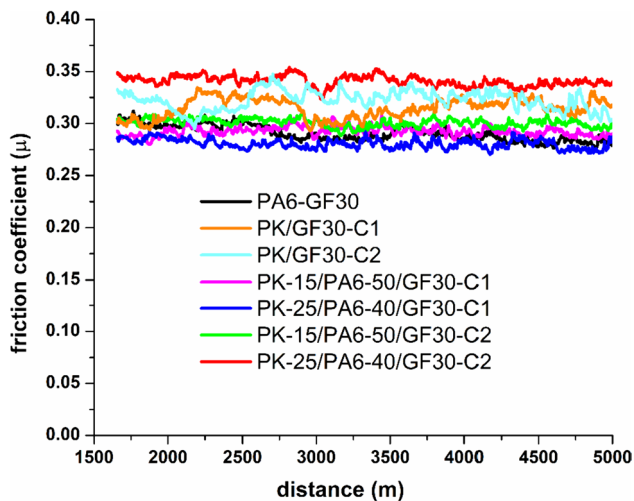
### 3.3 Tribological properties

The wear factors and friction coefficients of the 30% glass-fiber-reinforced PK/PA-6 blend composites were measured using the UTG Tribolog brand test device in accordance with the ASTM-G99 standard. The wear test parameters were set at a 40 N load, a 400-rpm sliding speed, and a 5000 m sliding distance. The wear test results including the friction coefficient and specific wear rate were obtained by selecting a specific section from the plates and were summarized in Table 5. A relationship between the friction coefficient and sliding distance of PK/GF-30, PA-6/GF-30, and PK/PA-6/GF30 blend composites with a constant abrasion velocity is plotted in Fig. 5. As can be seen in Fig. 5, the friction coefficients of all samples were stabilized after a sliding distance of 1500 m. The friction coefficients of PK/GF-30-C1 and PK/GF-30-C2 composites determined as 0.340 and 330 μ, were higher than the friction coefficient of neat PA-6/GF30 (0.289 μ) sample. After the melt blending process, the 30% glass-fiber-reinforced PK/PA-6 blend composites exhibited friction coefficients ranging from 0.286

**Table 5** Thermal and tribology properties of 30% glass-fiber-reinforced PK/GF30, PA-6/GF30, and PK/PA-6 blend composites

Sample	$T_{g1}$ (°C)	$T_{g2}$ (°C)	$T_m$ (°C)	Friction coefficient ( $\mu$ )	Specific wear rate ( $10^{-6}$ mm <sup>3</sup> /Nm)
PK/GF30-C1	15.6	–	219.6	0.340	1.83
PK/GF30-C2	15.2	–	221.3	0.330	1.81
PA-6/GF30	51.8	–	222.7	0.289	1.11
PK-15/PA6-50/ GF30-C1	15.3	50.4	222.1	0.298	1.55
PK-25/PA6-40/ GF30-C1	17.4	48.7	222.0	0.286	1.43
PK-15/PA6-50/ GF30-C2	15.6	49.9	221.9	0.302	1.14
PK-25/PA6-40/ GF30-C2	17.7	48.5	221.9	0.341	1.15

Tribological test was conducted three times to confirm reproducibility

**Fig. 5** The friction coefficient as a function of sliding distance for PA-6/GF30, PK/GF30-C1, PK/GF30-C2, PK-15/PA6-50/GF30-C1, PK-25/PA6-40/GF30-C1, PK-15/PA6-50/GF30-C2, and PK-25/PA6-40/GF30-C2 samples

to 0.341  $\mu$ . Compared to the neat PA-6/GF-30, the friction coefficients of the PK/PA6/ GF30 blend composites were generally increased by PK ratio from 15 to 25%. The PK-25/PA6-40/ GF30-C1 sample only displayed a lower friction coefficient than the neat PA-6/GF-30. This could be due to the insufficient performance of the C1 compatibilizer, stated in the SEM results. On the other hand, the PA-6/GF30 sample displayed higher wear resistance compared to the PK/GF30-C1 and PK/GF30-C2 samples. The  $T_g$  of PK (15.2 °C) was lower than that of PA-6 (51.8 °C), causing the PK to begin softening before the PA-6 under the wear test conditions. Therefore, the PA-6 had the capability to generate an adhesive transfer film during sliding, which prevented direct contact between the surfaces of PA-6/GF30 and metal pin. This mechanism reduced abrasive action, resulting in high wear resistance [28, 29]. Therefore, the specific wear rates of PK/PA6/ GF30 blend composites gradually increase upon addition of the PK, and the lowest specific wear rate was obtained for the PK-15/PA6-50/ GF30-C2 sample ( $1.14 \cdot 10^{-6}$

mm<sup>3</sup>/Nm) [28, 30]. Additionally, the blend composites prepared with C2 compatibilizer exhibited lower specific wear rates compared to those of C1 samples, irrespective of their compositions. These results indicate that the compatibility of C2 was more appropriate than that of C1, as supported by mechanical, thermal, and SEM data.

## 4 Conclusions

Herein, we demonstrated the effect of PK/PA-6 feed ratio and compatibilizer type (C1 and C2) on the mechanical, thermal, and tribological properties of 30% glass-fiber-reinforced blend composites. The mechanical properties of the PK/PA-6/GF-30 blend composites were recorded in between those of the PK/GF30 and the PA-6/GF30 composites. The tensile, flexural, and impact tests results indicated that the C2 was more appropriate than the C1 to enhance the compatibility between glass fibers with PK and PA-6 matrix, attributed to the maleic anhydride functionality. The SEM analysis revealed that the formation of a cohesive interface between glass fibers and the polymer matrix, with minimal fiber pullout, demonstrated the effectiveness of C2 in improving interfacial bonding. Thermal analysis demonstrated a slight decrease in both  $T_g$  and  $T_m$  values after the incorporation of the C1 and C2 compatibilizers. The  $T_g$  changes were more pronounced with C2, attributed to its maleic anhydride functionality promoting better adhesion between glass fiber and two phases. The tribological analysis highlighted the stabilized friction coefficients of all samples after a sliding distance of 1500 m. Additionally, the friction coefficients and specific wear rates of PK/PA6/GF30 blend composites were improved by increasing PK segment. The PK-25/PA6-50/GF30-C2 sample displayed a friction coefficient of 0.341  $\mu$  and a specific wear rate of  $1.15 \cdot 10^{-6}$  mm<sup>3</sup>/Nm. These results indicated that the compatibility of the C2 was more suitable than the C1, as supported by mechanical, thermal, microscopic, and tribology analyses. In summary, the type of compatibilizer enhanced the performance of glass-fiber-reinforced PK and PK/PA-6 blend composites,

providing valuable insights for the development of high-performance materials with tailored mechanical, thermal, and tribological properties.

**Acknowledgements** One of the authors (I.N.U.) thanks the Scientific Research Fund of Yalova University (Project No. 2022/DR/003) for the financial support.

## Declarations

**Conflict of interest** The authors have no conflicts of interest to disclose.

## References

1. Y.S. Jung, A. Canlier, T.S. Hwang, *Polymer* **141**, 102 (2018)
2. Y. Yang, S.-Y. Li, R.-Y. Bao, Z.-Y. Liu, M.-B. Yang, C.-B. Tan, W. Yang, *Polym. Int.* **67**, 1478 (2018)
3. A. Asano, M. Nishioka, Y. Takahashi, A. Kato, S. Hikasa, H. Iwabuki, K. Nagata, H. Sato, T. Hasegawa, H. Sawabe, *Macromolecules* **42**, 9506 (2009)
4. A. Kato, M. Nishioka, Y. Takahashi, T. Suda, H. Sawabe, A. Isoda, O. Drozdova, T. Hasegawa, T. Izumi, K. Nagata, *J. Appl. Polym. Sci.* **116**, 3056 (2010)
5. Y. Zhai, Y. Luo, X. Wang, C. Zhang, P. Deng, H. Chen, R. Zhang, R. Bao, Y. Zhou, M. Yang, *Polymer* **259**, 125324 (2022)
6. T. Zhang, H.-J. Kang, *Polymers* **13**, 3403 (2021)
7. F. Lin, Y. Liu, L. Song, X. Hao, X. Liu, S. Fan, Y. Wu, L. Mao, *J. Appl. Polym. Sci.* **138**, 50501 (2021)
8. Y. Wang, D.-F. Hou, K. Ke, Y.-H. Huang, Y. Yan, W. Yang, B. Yin, M.-B. Yang, *Polymer* **212**, 123173 (2021)
9. Y. Son, S. Lee, *J. Polym. Res.* **30**, 33 (2022)
10. S. Li, Y. Yang, X. Zha, Y. Zhou, W. Yang, M. Yang, *Nanomaterials* **8**, 932 (2018)
11. E. Marklund, U.W. Gedde, M.S. Hedenqvist, G. Wiberg, *Polymer* **42**, 3153 (2001)
12. X. Lu, K.Y. Lim, F.Y. Lim, L. Liu, S.-C. Wong, J. Zhao, *Plast. Rubber Compos.* **31**, 147 (2002)
13. F. Tang, Y.G. Jeong, *Polymer* **257**, 125281 (2022)
14. J.G. Bonner, *Polymer blends of PVC and polyketones*, SRI International Inc, US Patents 5610236 (1997).
15. J. Kim, S. Oh, S.M. Cho, J. Jun, S. Kwak, *J. Appl. Polym. Sci.* **137**, 49537 (2020)
16. I. Jeon, M. Lee, S.W. Lee, J.Y. Jho, *Macromol. Res.* **27**, 827 (2019)
17. I. Jeon, S.W. Lee, J.Y. Jho, *Macromol. Res.* **27**, 821 (2019)
18. S. Li, W. Wang, L. Yu, Z. Xia, X. Li, *J. Appl. Polym. Sci.* **135**, 46429 (2018)
19. G.R. Arpitha, N. Jain, and A. Verma, *Biomass Conversion and Biorefinery*, 1 (2023).
20. G.R. Arpitha, A. Verma, M.R. Sanjay, S. Siengchin, *Advances in Civil Engineering Materials* **10**, 427 (2021)
21. Y. Kim, J.W. Bae, C.S. Lee, S. Kim, H. Jung, J.Y. Jho, *Macromol. Res.* **23**, 971 (2015)
22. B.J. Lommerts, *Adv. Ind. Eng. Polym. Res.* **5**, 70 (2022)
23. Y. Kim, C.S. Lee, S. Kim, H. Jung, J.Y. Jho, *Macromol. Res.* **23**, 965 (2015)
24. J. Bae, B.C. Kim, *Macromol. Res.* **22**, 1165 (2014)
25. S.C. Tjong, S.-A. Xu, R.K.-Y. Li, Y.-W. Mai, *Compos. Sci. Technol.* **62**, 831 (2002)
26. H.C. Lee, Y. Son, S. Lee, *J. Appl. Polym. Sci.* **137**, 48743 (2020)
27. Y. Son, S. Lee, *J. Polym. Res.* **30**, 33 (2023)
28. Z. Chen, T. Li, Y. Yang, X. Liu, R. Lv, *Wear* **257**, 696 (2004)
29. S. Zhou, Q. Zhang, J. Huang, D. Ding, *J. Thermoplast. Compos. Mater.* **27**, 977 (2014)
30. Z. Chen, T. Li, X. Liu, and R. Lü, *J. Polym. Sci., Part B: Polym. Phys.*, **43**, 2514 (2005).

**Publisher's Note** Springer Nature remains neutral with regard to jurisdictional claims in published maps and institutional affiliations.

Springer Nature or its licensor (e.g. a society or other partner) holds exclusive rights to this article under a publishing agreement with the author(s) or other rightsholder(s); author self-archiving of the accepted manuscript version of this article is solely governed by the terms of such publishing agreement and applicable law.

## Authors and Affiliations

Irem Nehir Uysal<sup>1,2</sup> · Mehmet Atilla Tasdelen<sup>1</sup> 

✉ Mehmet Atilla Tasdelen  
tasdelen@yalova.edu.tr

<sup>1</sup> Faculty of Engineering, Department of Polymer Materials Engineering, Yalova University, 77200 Yalova, Turkey

<sup>2</sup> Department of Polymer Materials Engineering (MSc), Institute of Graduate Studies, Yalova University, 77200 Yalova, Turkey